Except near cutoff, the nominal width of a frequency bin centered at f is

$$\frac{c}{2ns\beta(f)} \simeq \frac{c}{2L\beta(f)}.$$

Thus, say, a device which uses an air dielectric waveguide and which is to achieve a resolution of 100 MHz needs to be a little more than 2 m long when operated midband ($f \simeq 1.5\, f_c$). The use of a dielectric with higher index would allow a shorter waveguide.

Now consider the undesired output term S_k^s. Its amplitude dependence on k is of the form

$$\frac{\sinh[n(j\pi k/N \pm \gamma s)]}{\sinh(\pi k/N \pm \gamma s)}$$

which peaks when k is a multiple of N and is small elsewhere. Thus, this term only interferes with at most a few of the usable values of k. To avoid such interference, the range of inputs must be slightly curtailed, so that slightly less than $n/2$ resolution cells may be covered.

Although the system was described above using rectangular waveguide, any other guiding medium, such as stripline, would do. Dielectrics with slow propagation velocity may be used to decrease the size of the apparatus.

One of the crucial questions to be investigated is whether the detector coupling can be achieved without introducing significant reflections. Such reflections would be misinterpreted as new frequency components.

Several generalizations of the above system are possible. One such modification is to include weighting of the autocorrelation samples to provide more desirable crosstalk characteristics. By weighting these terms, the function W may be given lower side lobes at the expense of a wider center lobe.

Another observation is that the integrators need not be strict integrators as described, but can be simpler low-pass filters. (The filtering may occur naturally as the detector response.) Further, these low-pass filter outputs need not be sampled and held, but need only be sampled by the analog multiplexer.

IV. Conclusion

A scheme of performing spectrum analysis over large bandwidths has been presented and briefly examined. Engineering questions, such as the ability to couple energy into the detectors without causing significant perturbations and the dynamic range limits imposed by the detectors, have yet to be addressed.

The approach allows simultaneous monitoring of all frequency bins within the band of interest and, unlike IFM methods, can operate with multifrequency inputs. The proposed scheme does not suffer from the bandwidth limit imposed by acoustooptic input devices or the bandwidth limit imposed by output sampling in compressive receivers. The approach also overcomes the slowness and ambiguity of scanning methods.

Acknowledgment

The author wishes to thank Dr. M. Damashek for discussions on this subject and Dr. D. E. Brown for his review of the manuscript.

References

[1] J. B.-Y Tsui, *Microwave Receivers With Electronic Warfare Applications* New York: Wiley, 1986

[2] N. E Goddard, "Instantaneous frequency-measuring receivers," *IEEE Trans. Microwave Theory Tech*, vol MTT-20, pp 292–293, Apr. 1972

[3] V. S Dolat *et al.*, "High-performance hybrid SAW chirp-Fourier-transform system," in *Proc 1978 Ultrasonics Symp*, September 25–27, 1978, pp 527–532

[4] R C. Williamson, "Reflection grating filters," in *Surface Wave Filters*, H. Mathews, Ed New York: Wiley, 1977, pp. 381–442

[5] H. M Gerard, "Surface wave interdigital electrode chirp filters," in *Surface Wave Filters*, H Mathews, Ed New York: Wiley, 1977, pp. 381–442

[6] G. K Montress and T. M Reeder, "A high performance SAW/hybrid component Fourier transform convolver" in *Proc 1978 Ultrasonics Symp.*, Sept 25–27, 1978, pp. 538–542.

[7] B. Lambert, "Wideband instantaneous spectrum analyzers employing delay line modulators," *IRE National Convention Record*, vol. 10, part 6, pp 69–78, Mar. 1962

[8] D. L Hecht, "Broadband acousto-optic spectrum analysis," in *Proc IEEE Ultrasonics Symp.* (Monterey, CA), Nov. 1973.

[9] T Turpin, "Spectrum analysis using optical processing," *Proc. IEEE*, vol 69, pp. 79–92, Jan. 1981.

[10] P. Kellman, H. N Shaver, and J. W Murray, "Integrating acousto-optic channelized receivers," *Proc. IEEE*, vol. 69, pp 93–100, Jan. 1981

[11] A. Vander Lugt, "Interferometric spectrum analyzer," *Appl. Opt*, vol. 20, no. 16, pp 2770–2779, 15 Aug 1981

[12] G A. Vanesse and H Sakai, "Fourier spectroscopy," in *Progress in Optics*, vol VI, E Wolf, Ed. Amsterdam: North-Holland, 1967, pp 261–330.

[13] R. C Milward, "Recent advances in commercial Fourier spectrometers for the submillimeter wavelength region," *IEEE Trans. Microwave Theory Tech*, vol MTT-22, pp 1018–1023, Dec 1974.

Modeling of Arbitrarily Shaped Signal Lines and Discontinuities

BARRY J. RUBIN, MEMBER, IEEE

***Abstract*—The propagation characteristics for signal lines and discontinuities embedded in a homogeneous medium and having any shape composed of steps along the Cartesian coordinates are obtained through an extension of the author's work on scattering from periodic apertures. The approach is specifically applied to high-performance computer packages, where previously employed capacitance and inductance techniques may not be appropriate. Numerical results are given for representative structures that involve signal lines, mesh planes, vias, and crossing and coupled lines.**

I. Introduction

Techniques for analyzing uniform transmission lines [1], [2] and discontinuities of regular shape [3] are well known. Unfortunately, a general solution technique has not existed for nonuniform lines or 3-D discontinuities of irregular shape, although it would be invaluable for analyzing computer modules [4], where signal lines bend and numerous discontinuities are encountered in the path between chips.

A section of such a module (Fig. 1) shows a signal line situated between mesh reference planes and connected to a second signal line through a via. Vias, stubs, right angle bends, and adjacent but nontouching other lines and vias represent discontinuities. The delay and impedance of, and coupling between, these structures must be determined so reflections that cause circuits to falsely switch can be avoided [5].

Various quasi-static and quasi-TEM approaches [6], [7] may be applied, but only to pieces of the problem. A more general approach involves three-dimensional capacitance and inductance

Manuscript received January 10, 1988; revised December 9, 1988

The author is with the Thomas J. Watson Research Center, IBM Corporation, Yorktown Heights, NY 10598.

IEEE Log Number 8927158.

0018-9480/89/0600-1057$01.00 ©1989 IEEE

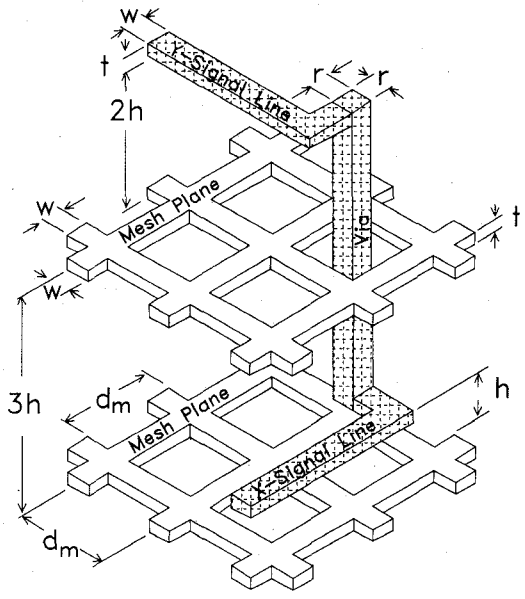

Fig. 1. Section of multichip module showing reference planes and signal lines interconnected through a via.

calculation [8], [9], but the inherent circuit approximations [10] may lead to inaccuracies. Our purpose here is to describe a guided wave solution that does not suffer from the above limitations, to demonstrate it on a few representative structures, and to discuss convergence and other practical considerations.

II. Solution Technique

The structure, to be consistent with the solution technique, must first be represented as periodic along x and y, with x the direction chosen for propagation. The propagation characteristics will then be determined from the propagation constant and current distribution.

The structure is thus represented by a unit cell. The periodicity along x not only makes propagation possible, but also eliminates specification of end regions, whose presence in finite structures may obscure the propagation characteristics sought. The periodicity along y, however, gives rise to coupling between unit cells that is generally undesirable but can be minimized. For instance, if we wish to analyze an isolated signal line above a mesh plane, we define a unit cell having y periodicity much greater than the signal line's height above the mesh plane so that the coupling between signal lines is small. If we wish to model two adjacent signal lines, then signal line positions within the unit cell, along y, are intentionally left vacant. Thus, coupling is essentially limited to those adjacent lines that reside in the same unit cell.

As described in [11], the current in the unit cell is approximated as a linear combination of coefficients multiplied by rooftop shape functions [12] (Fig. 2) and a complex phase factor that involves the propagation constant. Current continuity at the edges is ensured through half-rooftop functions that form corner functions. At junctions of planes, two or three corner functions unambiguously represent the current. The electric field, obtained through application of the Floquet condition and standard Fourier series techniques, is integrated and tested over line segments to satisfy the electric field boundary condition.

The resulting eigenvalue problem [13] is solved first for the propagation constant, using a Newton search, and then for current distribution. Voltages, which are path dependent for non-TEM structures, are calculated by integrating the electric

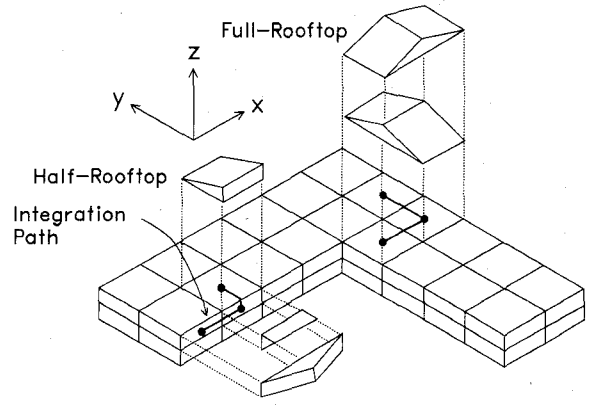

Fig. 2. A section of a unit cell which shows rooftop elements and integration paths for a mesh plane ($S_x = 6$, $S_y = 6$, $S_z = 2$).

field. Effective values of per-unit-length capacitance C and inductance L may be calculated, for lossless structures, through $t_0 = \sqrt{LC}$ and $Z_0 = \sqrt{L/C}$, where Z_0 is the characteristic impedance (obtained from the voltage and current) and t_0 is the delay (obtained from the propagation constant). By analyzing signal lines with and without discontinuities, equivalent circuits for the discontinuities may be inferred. For instance, to model a via running through a ground plane, signal lines with and without such vias would be analyzed. The difference in C gives the via's capacitance and the difference in L gives the via's inductance.

III. Unit Cells Defined for Computer Module

The computer module considered (Fig. 1) involves mesh planes that have period d_m along x and y, thickness t, and are formed from overlapping strips having the same width w and thickness as the signal lines. Signal lines and mesh planes, vertically separated by distance h, are so aligned that their projections on the plane $z = 0$ coincide, while vias have square cross section, side r, and are centered with respect to the mesh openings.

For each structure we define a new unit cell, having respective periodicities d_1 and d_2 along x and y, that is subdivided into S_x, S_y, and S_z intervals along x, y, and z [11]. The unit cell section of Fig. 2, which for simplicity shows only one period of a mesh plane so that $d_1 = d_2 = d_m$, is subdivided according to $S_x = S_y = 6$ and $S_z = 2$. The conductors are hollow, lossless, and situated in free space. Results are calculated at low frequency, where the dispersion curves are linear. The characteristic impedance is calculated between facing conductor surfaces along indicated paths and the delay is normalized to that of light.

IV. Results and Discussion

The algorithm employed to generate the matrix in the eigenvalue problem is a version of the one described in [11], but adapted for propagation. Enhancements were needed to reduce analysis time to only minutes on a general-purpose mainframe computer, as even the simplest 3-D structures of interest require repeated calculation (because of the Newton search) of a large matrix. These enhancements include truncation, in appropriate matrix elements, of space harmonics highly attenuated along z and improvements in the table lookup facility. For most cases, the run time is determined by the Gauss elimination, not the matrix setup.

We first consider convergence, determining the number of subsections (or grid size) needed for reasonable accuracy. For a signal line above a single mesh plane ($d_1 = d_2 = d_m = 1.0$ mm,

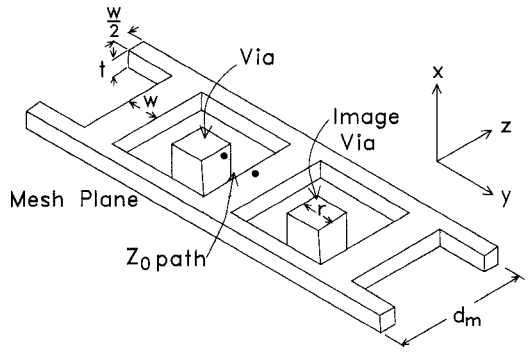

Fig. 3. Unit cell for via running through infinite array of mesh planes.

TABLE I
PROPAGATION CHARACTERISTICS FOR VIA STRUCTURE OF FIG. 3

t (mm)	t_0	$Z_0(\Omega)$	C(pF/cm)	L(nH/cm)
no mesh	1.000	103.21	0.322	3.44
0.0625	1.236	80.54	0.511	3.32
0.1250	1.250	76.58	0.544	3.19
0.2500	1.271	69.51	0.610	2.94
0.5000	1.263	57.67	0.730	2.43
0.7500	1.194	46.73	0.852	1.86
1.0000	1.000	36.46	0.914	1.23

$d_1 = d_m = 1.0$ mm, $d_2 = 3.0$ mm, $w = 0.50$ mm, $r = 0.25$ mm, S_x varies, $S_y = 24$, $S_z = 8$.

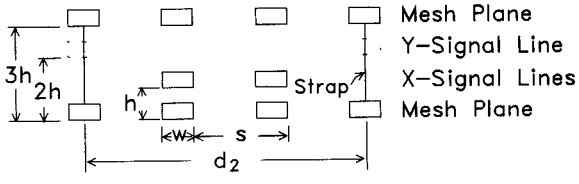

Fig. 4. Unit cell for coupled signal lines situated between mesh reference planes

$w = 0.25$ mm, $t = 0.1$ mm, $h = 0.5$ mm) the grid $S_x = S_y = 4$, $S_z = 6$ yields a t_0 of 1.0374 and a Z_0 of 221.1 Ω. Overall changes of less than 0.3 percent in t_0 and 2.0 percent in Z_0 were observed when the grid size was gradually reduced until $S_x = S_y = 16$, $S_z = 12$ was reached. Between 84 and 474 rooftop currents were needed, with corresponding computation times on an IBM 3090 of 0.2 min and 4.2 min. An equivalent but zero-thickness structure, over the same range in S_x and S_y, displays relatively poor convergence, as indicated by a t_0 that ranges from 1.0627 to 1.0494 and a Z_0 that ranges from 311 Ω to 284 Ω. The above indicates that even a coarse grid is satisfactory for structures that have thickness.

Fig. 3 shows a via running through an infinite array of mesh planes, with guiding made possible by an image via that carries return current. Here, the mesh planes lie in the $y-z$ plane, with the distance between mesh planes given by d_1. The via's impedance and delay can be used to find the reflection that occurs when a wave exits a signal line to travel vertically within the module. Table I shows that Z_0 decreases with mesh plane thickness, but that t_0 remains fairly constant. Calculated from Z_0 and t_0, C increases with thickness but L, because of surface eddy current, decreases about as fast. The entries no mesh and $t = 1$ mm, where the mesh acts as a continuous rectangular enclosure, represent TEM cases. Two-dimensional calculations, through procedures described in [1], show respective capacitances of 0.324 pF/cm and 0.904 pF/cm, agreement so close to give confidence for the nonuniform cases.

TABLE II
CHARACTERISTICS FOR COUPLED LINE STRUCTURE OF FIG. 4

refer plane	y line	mode	t_0	Z_0 (Ω)	C (pF/cm)	L (nH/cm)	C_{11} (pF/cm)	C_{12} (pF/cm)	L_{11} (nH/cm)	L_{12} (nH/cm)
mesh	no	even	1.017	74.42	0.456	2.523	0.476	0.0207	2.393	0.130
mesh	no	odd	1.006	67.47	0.497	2.262				
mesh	yes	even	1.098	67.30	0.544	2.463	0.556	0.0116	2.328	0.135
mesh	yes	odd	1.058	62.19	0.567	2.193				
solid	no	even	1.001	69.00	0.483	2.301	0.499	0.0153	2.232	0.069
solid	no	odd	1.000	64.87	0.514	2.162				
solid	yes	even	1.068	62.93	0.566	2.240	0.574	0.0078	2.169	0.071
solid	yes	odd	1.048	60.06	0.582	2.098				

$d_1 = d_m = 3.0$ mm, $d_2 = 9.0$ mm, $w = h = s = 1.0$ mm, $t = 0.5$ mm, $S_x = 3$, $S_y = 36$, $S_z = 7$

Coupled signal lines situated between reference planes, with and without crossing y-signal lines, are considered in Fig. 4. The unit cell has two x-signal lines, separated by distance $s = d_1$, with one signal line position intentionally left vacant. To preclude multiple even modes (two reference planes and a signal line, each continuous along x, support two modes) but minimally alter the field, a zero-thickness strap (width 1.0 mm and aligned with the y-directed mesh strips) is inserted between the mesh planes.

Table II gives the propagation characteristics for both solid and mesh reference planes. Symmetry along y permits an even- and odd-mode analysis. The self- and coupling capacitances, C_{11} and C_{12}, and the self- and coupling inductances, L_{11} and L_{12}, are listed between the entries for even and odd modes. Two-dimensional calculation for the solid case with no y-lines gives $C_{11} = 0.503$ pF/cm, $C_{12} = 0.0152$ pF/cm, $L_{11} = 2.211$ nH/cm, and $L_{12} = 0.0668$ nH/cm. The agreement is excellent. Near-end coupled noise and far-end coupled noise (due to contra- and codirectional coupling), which depend respectively on the sum and difference of the capacitive and inductive coupling coefficients, may then be calculated. Crossing y-signal lines, through significant decrease in capacitive coupling, respectively decrease near-end but increase far-end noise. The mesh, providing less shielding and greater nonuniformity than a solid plane, increases both noises. Structures which are nonsymmetric or have more than two signal lines cannot be described through even- and odd-mode quantities but can be alternatively handled [13].

V. DISCUSSION

A sample of signal line and discontinuity structures that are found in computer modules have been characterized. The excellent agreement shown, for those cases that lend themselves to two-dimensional analysis, gives us confidence in the results for those structures that cannot otherwise be accurately modeled. Based on this agreement and the rapid convergence observed for 3-D signal lines, accurate results can be obtained with even a coarse grid. In a comprehensive characterization of a multichip computer module, which the author plans to report on, convergence and expected results were observed for structures requiring over 2000 current elements.

Though not considered here, transmission lines having helix or other shape can be analyzed (even at frequencies where quasi-TEM approaches break down) as can non-TEM waveguides and

their discontinuities. Nonuniform grids or layered dielectrics can be included [14], but would substantially increase the algorithm's number of nonredundant table lookup elements, increasing storage requirements and run time. By representing the conductors as a honeycomb, with internal planes having finite sheet resistance, solid structures having even anisotropic resistance can be handled. Though the additional rooftop elements increase computational effort, a wide variety of problems involving skin effect could be accommodated.

REFERENCES

[1] W. T Weeks, "Calculation of coefficients of capacitance of multiconductor transmission lines in the presence of a dielectric interface," *IEEE Trans. Microwave Theory Tech.*, vol MTT-18, pp. 35–43, Jan. 1970

[2] W T Weeks, L. L Wu, M. F McAllister, and A Singh, "Resistive and inductive skin effect in rectangular conductors," *IBM J. Res. Develop*, vol. 23, no 6, pp. 652–660, Nov. 1979.

[3] N. Marcuvitz, *Waveguide Handbook* (M I T Rad Lab. Series, vol 10) New York: McGraw-Hill, 1951.

[4] A. J Blodgett and D. R. Barbour, "Thermal conduction module: A high performance multilayer ceramic package," *IBM J. Res. Develop*, vol 26, no. 1, pp 30–36, Jan. 1982.

[5] E E. Davidson, "Electrical design of a high speed computer package," *IBM J Res Develop.*, vol. 26, no. 3, pp 349–361, May 1982.

[6] T. Sugiura, "Analysis of distributed-lumped strip transmission lines," *IEEE Trans. Microwave Theory Tech.*, vol. MTT-25, pp. 656–661, Aug. 1977.

[7] T. Wang, R. F. Harrington, and J. R. Mautz, "Quasi-static analysis of a microstrip via through a hole in a ground plane," *IEEE Trans Microwave Theory Tech*, vol. 36, pp. 1008–1013, June 1988.

[8] A. E Ruehli and P. A. Brennan, "Efficient capacitance calculations for three dimensional multiconductor systems," *IEEE Trans. Microwave Theory Tech.*, vol. MTT-21, pp. 76–82, Feb 1973.

[9] A. E. Ruehli, "Inductance calculations in a complex integrated circuit environment," *IBM J. Res. Develop.*, vol 16, no. 5, pp 470–481, Sept. 1972.

[10] A. E Ruehli, "Equivalent circuit models for three-dimensional multiconductor systems," *IEEE Trans. Microwave Theory Tech*, vol. MTT-22, pp. 216–220, Mar 1974.

[11] B. J. Rubin, "Scattering from a periodic array of apertures or plates where the conductors have arbitrary shape, thickness, and resistivity," *IEEE Trans. Antennas Propagat.*, vol. AP-34, pp. 1356–1365, Nov 1986.

[12] A. W. Glisson and D. R Wilton, "Simple and efficient numerical methods for problems of electromagnetic radiation and scattering from surfaces," *IEEE Trans. Antennas Propagat.*, vol. AP-25, pp. 593–607, Sept. 1980.

[13] B. J Rubin, "The propagation characteristics of signal lines in a mesh-plane environment," *IEEE Trans. Microwave Theory Tech*, vol. MTT-32, pp 522–531, May 1984.

[14] C. H. Chan and R. Mittra, "The propagation characteristics of signal lines embedded in a multilayered structure in the presence of a periodically perforated ground plane," *IEEE Trans. Microwave Theory Tech.*, vol 36, pp. 968–975, June 1988.